How to cite: *Angew. Chem. Int. Ed.* **2022,** *61,* e202112842
International Edition: doi.org/10.1002/anie.202112842
German Edition: doi.org/10.1002/ange.202112842

Polypeptide Films

Crosslinked Polypeptide Films via RAFT-Mediated Continuous Assembly of Polymers

Nicholas J. Chan, Sarah Lentz, Paul A. Gurr, Shereen Tan, Thomas Scheibel, and Greg G. Qiao**

Abstract: *Polypeptide coatings are a cornerstone in the field of surface modification due to their widespread biological potential. As their properties are dictated by their structural features, subsequent control thereof using unique fabrication strategies is important. Herein, we report a facile method of precisely creating densely crosslinked polypeptide films with unusually high random coil content through continuous assembly polymerization via reversible addition–fragmentation chain transfer (CAP-RAFT). CAP-RAFT was fundamentally investigated using methacrylated poly-L-lysine (PLLMA) and methacrylated poly-L-glutamic acid (PLGMA). Careful technique refinement resulted in films up to 36.1 ± 1.1 nm thick which could be increased to 94.9 ± 8.2 nm after using this strategy multiple times. PLLMA and PLGMA films were found to have 30–50 % random coil conformations. Degradation by enzymes present during wound healing reveals potential for applications in drug delivery and tissue engineering.*

Introduction

For decades, scientists have been deeply fascinated in surface modification via the introduction of synthetic polypeptides for a wide range of applications including biosensing,[1] active molecule release[2] and antibiofouling/antimicrobial applications.[3] Polypeptides can be designed to bear application specific chemical and physical properties which largely is afforded by their ability to fold into different well-defined conformations known as secondary structures based on their specific amino acid sequence.[4] Thus, the design and manipulation of secondary structures (e.g. α-helices, β-sheets, random coils) forms a core directive for material scientists.[5] While conventional techniques for coatings and film formation are well established, synthetic polypeptides formed through *N*-carboxyanhydride ring-opening polymerization (NCA ROP) offers the opportunity to lean into grafting polymerization techniques for the fabrication of polypeptide films.[6] Grafting-to and grafting-from strategies both result in linear polymers with a terminal group anchored to the surface.[7] However, films formed through grafting-to techniques tend to be limited by steric hindrance associated with tethering a large molecule to a surface, while films fabricated through a grafting-from approach are difficult to characterize after more than one monomer is introduced to the system.[7] Grafting-through strategies aim to mitigate these issues, by using macromonomers with polymerizable end groups, instead of monofunctional monomers resulting in thicker films with well-defined polymer bottlebrushes.[3a,8] With all the advantages that result from using grafting-through methods, our group has developed a unique methodology, which yields unique, robust, crosslinked films, called continuous assembly polymerization (CAP).[9]

As with grafting-through techniques, CAP utilizes polymers with a polymerizable group, but unlike traditional grafting-through techniques, these polymerizable groups are not restricted to a singular endgroup resulting in a macrocrosslinker.[10] The result is a dense crosslinked polymeric network forming a robust film on the substrate surface with often a unique morphology, compared to even traditional grafting through methods. The technique itself is robust enough that multiple other macrocrosslinkers have already been utilized using this technique such as polyethyleneglycol (PEG)-based,[11] 2-hydroxyethylacrylate (HEA)-based,[9a,c] and polythiophene[12] polymers. Uniquely, this can be combined with macrocrosslinkers which already bear unique morphologies. For example, polyrotaxane-based macrocrosslinkers have been utilized to afford a film with the densely crosslinked nature of CAP films, along with the stimuli sensitivity associated with the "host–guest" chemistry of a cyclodextrin-based polyrotoxane network.[13] The unique morphology afforded through CAP and the wide variety of macrocrosslinkers amenable to this process has enabled the synthesis of a range of films targeting a variety of different applications.[10a,11a] Antifogging qualities of a PEG-based film have been shown using this technique after exposure of the film at −20 °C to ambient conditions, and films retained high light transmittance with a relatively low crosslinking density.[11b] However, despite the aforemen-

[*] N. J. Chan, S. Lentz, P. A. Gurr, S. Tan, G. G. Qiao
Polymer Science Group, Department of Chemical Engineering
University of Melbourne
Parkville, Melbourne, Victoria 3010 (Australia)
E-mail: gregghq@unimelb.edu.au
N. J. Chan, S. Lentz, T. Scheibel
Lehrstuhl Biomaterialien
Universität Bayreuth
Prof.-Rüdiger-Bormann-Str. 1, 95447 Bayreuth (Germany)
E-mail: thomas.scheibel@uni-bayreuth.de

tioned versatility of polypeptides, they have yet to be utilized with this technique. In parallel to the established library of crosslinkers is the variety of techniques for CAP, which have since been established including various fabrication conditions.[9d] Recently a unique patterning method has been developed employing CAP through microcontact printing which involves delivering material via a polymeric stamp.[14] Alongside these advances, the development of CAP includes different polymerization methods such as ring-opening metathesis polymerization (ROMP)[12,13] and atom transfer radical polymerization (ATRP).[11] Fundamentally, the method of polymerization utilized impacts film properties due to the mechanistic differences and as such developing CAP using different polymerization techniques is of profound interest. A blue-light mediated system employed a thiocarbamate as a photoiniferter, but the film thickness's being limited to approximately 5 nm.[9a] It is this variability in properties that highlights the need for investigating, the as yet unreported, reversible addition–fragmentation chain transfer (RAFT) polymerization as a CAP technique.

RAFT is identified as one of the most robust and versatile reversible-deactivation radical polymerization techniques.[15] In a RAFT polymerization system, polymerization is controlled by the degenerative chain transfer of the chain transfer agent (CTA) in the form of a thiocarbonylthio compound (known as a RAFT agent) to the polymer chains, leading to the sequential insertion of monomer units to the initial RAFT agent.[15d,16] As initiation is still free-radical based, there are numerous approaches to RAFT polymerization including initiation through enzymes, thermal initiators or acoustic cavitation of bubbles in the system via ultrasound. However, for a surface-initiated polymerization, light-based RAFT techniques provide a facile method of yielding grafted polymers.[7c,17] Using our already developed techniques in both RAFT polymerization[18] and NCA ROP,[19] we aim to further develop the potential of CAP-RAFT while fabricating polypeptide-based films with secondary structure morphologies based on a fabrication technique rather than solely on polypeptide structure.

Herein, we expand on this film formation strategy, to perform blue light-mediated CAP-RAFT using synthetic polypeptide based macrocrosslinkers. This is the first instance of fabricating a chemically crosslinked NCA ROP/based polypeptide film with precision control of thickness in one-step, controlled multilayer structures with designed composition and specifically formed peptide secondary structure resulting from the fabrication technique itself rather than solely on the polypeptide structure. Photoinitiator lithium phenyl-2,4,6-trimethylbenzoylphosphinate (LAP) was used in conjunction with two different model RAFT agents. A dithiobenzoate and a trithiocarbonate with differing kinetics were chosen to investigate their influence on the ability to form thick uniform films. Furthermore, we investigated the importance of RAFT agent in solution, which historically has been required to develop films of uniform thickness and its effects on both kinetics and uniformity. In furthering this work, we also explored the ability to produce stratified, multi-layered cross-linked films by coupling RAFT agent to the initiating surface to re-initiate the CAP-RAFT process at the growing polymer surface. As a demonstration of versatility, a second polypeptide based macrocrosslinker was introduced into the system. In both cases, an unusually high random coil conformation was produced which, combined with the evident enzymatic degradation demonstrated, presents unique opportunities in drug delivery and tissue engineering.

Results and Discussion

Polypeptide macroinitiators were synthesized through NCA ROP, subsequent deprotection and methacrylation (Supporting Information Figure S1, S2). NCA ROP is known to be a facile method for creating long chain, non-sequence specific polypeptides.[4b,20] With a selection of 21 canonical amino acids with varying degrees of hydrophobicity, physical properties and chemical functionality, it makes them a highly versatile polymer class for a wide range of applications.[20b,21] To synthesize a model polypeptide macroinitiator, the homopolypeptide ε-carboxybenzyl-protected poly(L-lysine(Z)) (PZLL) was synthesized using hexylamine as the initiator. The use of PLL as the base polypeptide is rooted in its pendant amines which are ideal for material functionalization. The polypeptide was then treated with hydrobromic acid (HBr), removing the carboxybenzyl protecting group and revealing pendant primary amines of poly(L-lysine) (PLL) which would be amenable to methacrylation. This methacrylation was performed by first deprotonating the polypeptide in a 10 wt% aqueous solution by raising the pH to 10–11 and then addition of methacrylic anhydride, resulting in a methacrylation of 15 % (Supporting Information Table S1). It should be noted that increasing macrocrosslinker functionalization will generally yield increased film thickness when utilizing CAP as demonstrated in a previous study.[10c] However, 10 % of repeat units with double bonds is generally sufficient for CAP process. While this results in poly(L-lysine-*g*-methacrylate) (PLLMA) as intended, a fortuitous side-effect is that the polypeptide remains deprotonated allowing for CAP to be performed in organic solvents (Figure 1).

To prepare the surfaces for CAP, RAFT agent was immobilized onto aminated silica surfaces. Silica surfaces were aminated with 3-aminopropargyl triethoxysilane (APTES) using previously established methods.[22] The subsequent amine groups were susceptible to carbodiimide coupling with carboxylic acid-terminated RAFT agents (Supporting Scheme S3). To establish the validity of this method, 4-cyano-4-(phenylcarbonothioylthio)pentanoic acid (CPADB) was anchored as a model dithiobenzoate RAFT agent, allowing CAP-RAFT to be performed using PLLMA macrocrosslinker. CPADB has been used previously as a model dithiobenzoate RAFT agent for the study of methacrylamine monomers in solution,[23] and thus was deemed an appropriate model RAFT agent in this instance.

CAP-RAFT was performed by soaking the treated surfaces in a DMSO solution of PLLMA macrocrosslinker and LAP photoinitiator and irradiated under blue light

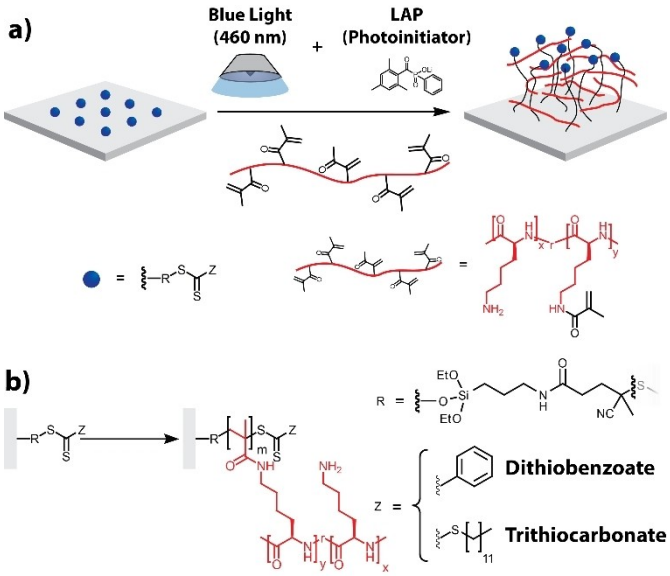

Figure 1. Schematic for CAP-RAFT using a polypeptide macroinitiator onto a surface functionalized with RAFT agent. a) Graphical schematic of CAP-RAFT of PLLMA macrocrosslinker through the use of blue light (4 mW cm^{-2}, λ_{max} = 460 nm). b) Chemical schematic representing the use of model dithiobenzoate and trithiocarbonate RAFT agents.

(4 mW cm^{-2}, $\lambda_{max} \approx 460$ nm). To confirm that film formation is due to CAP rather than solely adhesion of the macroinitiator to the surface, control experiments were performed with specific elements absent from the system (Supporting Information Table S2). All samples showed very small amount (1.31–5.60 nm) of film formation due to adhesion of deposited polypeptide. As would be expected, surfaces without surface initiator resulted in films of similar thicknesses, indicating a lack of surface confined polymerization (Figure 1). Furthermore, samples kept in the dark (i.e. no blue light exposure) also showed a lack of surface confined polymerization confirming the requirement for blue light for RAFT polymerization. Our group has previously shown that RAFT polymerization can be initiated with blue light without the use of a photoinitiator with a significantly lowered rate of polymerization, compared to other known RAFT mechanisms.[24] However, only samples with photoinitiator showed any evidence of polymerization, with film thickness of at least 30 nm observed, providing strong evidence of surface confined RAFT polymerization.

Previous papers have shown that surface initiated RAFT polymerization in general requires the use of a RAFT agent in solution to ensure consistent film thickness.[7c] Recently, Seo et al. demonstrated the use of SI-PET-RAFT without RAFT agent in the solution to yield patternable polymer brushes.[25] This is in agreement with our results indicating polymerization is confined to the film surface. Thus, to observe the degree of polymerization occurring both with and without RAFT agent in solution, analysis of the aggregate size was performed. DLS revealed an increase in particle size after irradiation under blue light as long as photoinitiator was present in solution (from 0.901 ± 0.0590 nm to 2.47 ± 0.210 nm with LAP and without functionalized surfaces) (Supporting Figure S6 and S7). A decrease in particle size correlating to a decrease in polymerization in the supernatant was observed with the introduction of functionalized surfaces, signifying an increase in control upon their introduction; for reactions without RAFT agent in solution, particles with a diameter of 2.47 ± 0.210 nm were observed after reaction without surfaces compared to 2.04 ± 0.360 nm with surfaces. With RAFT agent in solution, particles with a diameter of 4.01 ± 0.513 nm without surfaces were observed compared to 3.19 ± 0.41 nm with surfaces. However, the degree of polymerization in solution was found to be decreased without any free RAFT agent in solution signifying greater surface confinement of the reaction.

To further investigate the necessity of sacrificial RAFT agent when using polymeric macroinitiators, experiments with and without RAFT agent in solution were performed (Figure 2). In the presence of sacrificial RAFT agent, films were found to reach a maximum of 36.1 ± 1.1 nm after 16 h (Figure 2ai) with an RMS roughness of 6.1 nm (Figure 2aii). Without RAFT agent in solution, surfaces grew slower (24 h maximum), rougher and thinner (31.5 ± 2.4 nm with an RMS roughness of 9.4 nm), however remained relatively uniform in thickness, despite more regions of varied thickness (Figure 2b). In both cases, surfaces were found to have relatively high RMS roughness with respect to the film thickness. Furthermore, the overall homogeneity of the surface was found to be decreased without RAFT agent in solution. Though both films were relatively homogeneous, large regions with denser films were also observed. This has been observed in previous instances of the use of CAP which is due to the decreased availability of initiator at the film surface as it is covered by macrocrosslinker during film growth, with differences in homogeneity emerging based on the polymerization technique utilized and the macromonomers.[10] Furthermore, RAFT agents are susceptible to aminolysis by primary amines, potentially causing the degradation.[26] To determine if this was occurring, analysis of the supernatant after reaction both with and without RAFT agent in solution was performed. Dialysis was performed to remove excess CPADB (RAFT agent) and LAP, with the resulting ^{1}H NMR revealing splitting patterns consistent with aromatic rings which would only be present due to aminolysis of CPADB (Supporting Figure S8). Although solution experiments have confirmed that aminolysis can occur with PLLMA, direct confirmation on the surface is challenging due to the low concentration of the RAFT end groups. On the other hand, uneven growth of CAP layer can also be due to other reasons such as monomer type, polymerization methods as well as efficiency of re-initiation as observed before in other systems. Furthermore, while there is a relatively significant impact upon the introduction of RAFT agent in solution, it is not a crucial requirement in this system.

To observe if this trend remained consistent with other initiators, 4-cyano-4-[(dodecylsulfanylthiocarbonyl)sulfanyl]-pentanoic acid (CDTPA)—a trithiocarbonate-based RAFT agent—was introduced in the same manner as the dithiobenzoate initiator. Trithiocarbonates typically have a high

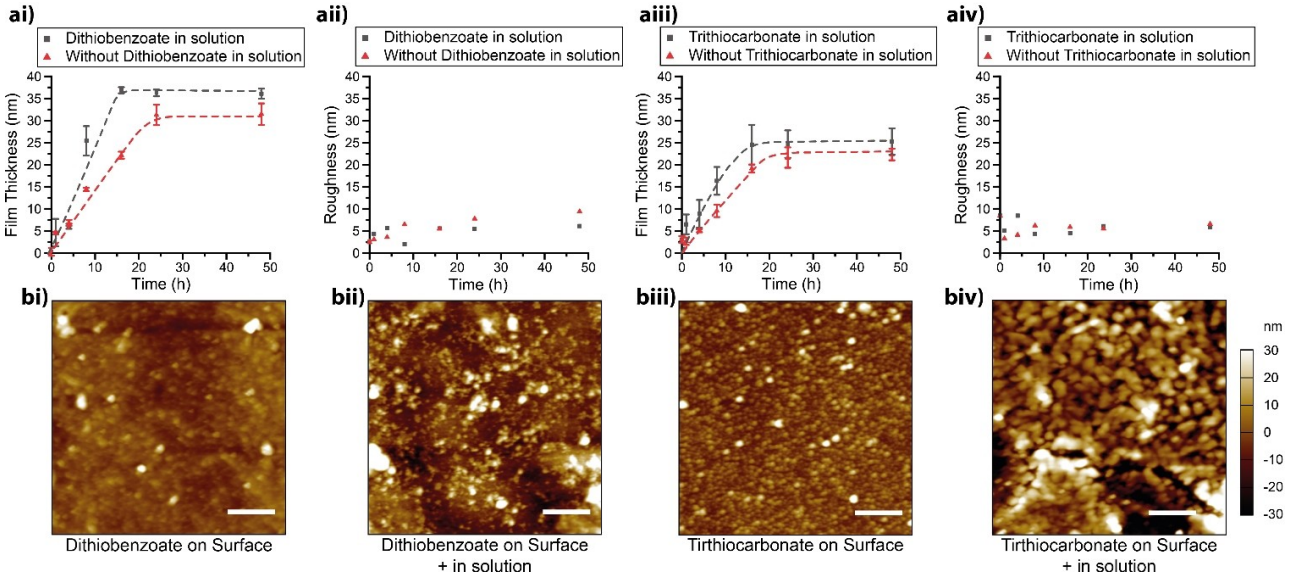

Figure 2. AFM imaging and analysis of CAP-RAFT films using a PLLMA macrocrosslinker utilizing different model RAFT agents. ai, aii) Analysis of film growth utilizing a dithiobenzoate RAFT agent observing kinetics of film growth (ai) and film roughness (aii) both with and without RAFT agent in solution. aiii, aiv) Analysis of film growth utilizing a trithiocarbonate RAFT agent observing kinetics of film growth (aiii) and film roughness (aiv) both with and without RAFT agent in solution. b) Surface morphology after 48 h of CAP-RAFT utilizing systems imaged using AFM with bi) a dithiobenzoate RAFT agent anchored to the surface as well as in RAFT agent in solution; bii) a dithiobenzoate RAFT agent anchored to the surface but not in the reaction solution; biii) a trithiocarbonate RAFT agent anchored to the surface as well as in RAFT agent in solution; and biv) a trithiocarbonate anchored to the surface but not in the reaction solution (scale bars = 1 μm).

affinity towards methacrylamides[27] and would provide some insight toward specific variability associated with using CAP (Figure 2). The time to reach maximum film thickness was the same as with the dithiobenzoate initiator, with and without sacrificial RAFT agent (16 h and 24 h respectively), but thicknesses were significantly reduced both with and without RAFT agent (25.3 ± 3.0 and 22.3 ± 1.3 nm respectively) (Figure 2a iii–iv). Furthermore, the morphologies of the films were found to have more significant aggregation (Figure 2b iii–iv). This appears to concur with the general principal that trithiocarbonates are known to be less active than their dithiobenzoate counterparts.[15d] However, they are less susceptible to aminolysis,[26c] supporting the hypothesis that the lower overall homogeneity of the dithiobenzoate samples is due to RAFT agent degradation by aminolysis. Nonetheless, as we aim to develop this method by keeping polymerization surface confined, we continued testing without RAFT agent in solution.

One advantage of CAP is the ability to increase the film thickness without concern for maintaining chain-end fidelity through re-initiation. As lysine residues have primary amine side chains, these films are uniquely susceptible to modification using the same carbodiimide chemistry employed for immobilization of the carboxylic acid-functional RAFT agent. From this RAFT agent-functionalized layer, a second layer of CAP could be performed (Figure 3a). This process could theoretically be continuously repeated to yield thicker films based on desired functionality. Using this strategy, we were able to grow films with 94.9 ± 8.24 nm in thickness after 4 layers (Figure 3b). It should be noted that a prominent increase in regions aggregation was also observed as more and more layers were introduced to the system (Figure 3d). Furthermore, these pendant primary amines are no longer available for carbodiimide coupling after attacking another immobilized RAFT agent. While this did not seem to have a significant effect on the first or second layers, this irregular morphology was much more pronounced in the third and fourth layers. Nonetheless, this demonstrates the potential to develop multilayered systems which can be increased further based on previous works demonstrating similar capabilities.[10]

With the use of polypeptides in the formation of these films comes the presence of secondary structures typical for proteins and polypeptides with poly-L-lysine being no exception.[28] ATR-FTIR spectra around the Amide I band (1600–1720 cm^{-1}) are often used to analyze the secondary structure content of proteins.[28] By observing this region of the spectra, the bottom three layers were found to share similar structures based on the major peaks (Figure 3c). However, the introduction of the fourth layer appeared to have a drastic effect with the peak at 1649 cm^{-1} splitting into two peaks (1658 and 1642 cm^{-1}) and a drop of the peak at 1696 cm^{-1} both indicating a drop in β-sheet formation.

To further determine the secondary structures present, lineshape analysis was performed according to Chirgadze et al.[29] for IR analysis of polypeptides. High molecular weight poly-L-lysine is well known to form random coils in solution while charged,[30] which is changed to a primarily α-helical structure under alkali aqueous conditions (i.e. uncharged primary amines).[28d] Poly-L-lysine films formed utilizing different methodologies including dip coating quartz in an alkali aqueous media or grafting the polypep-

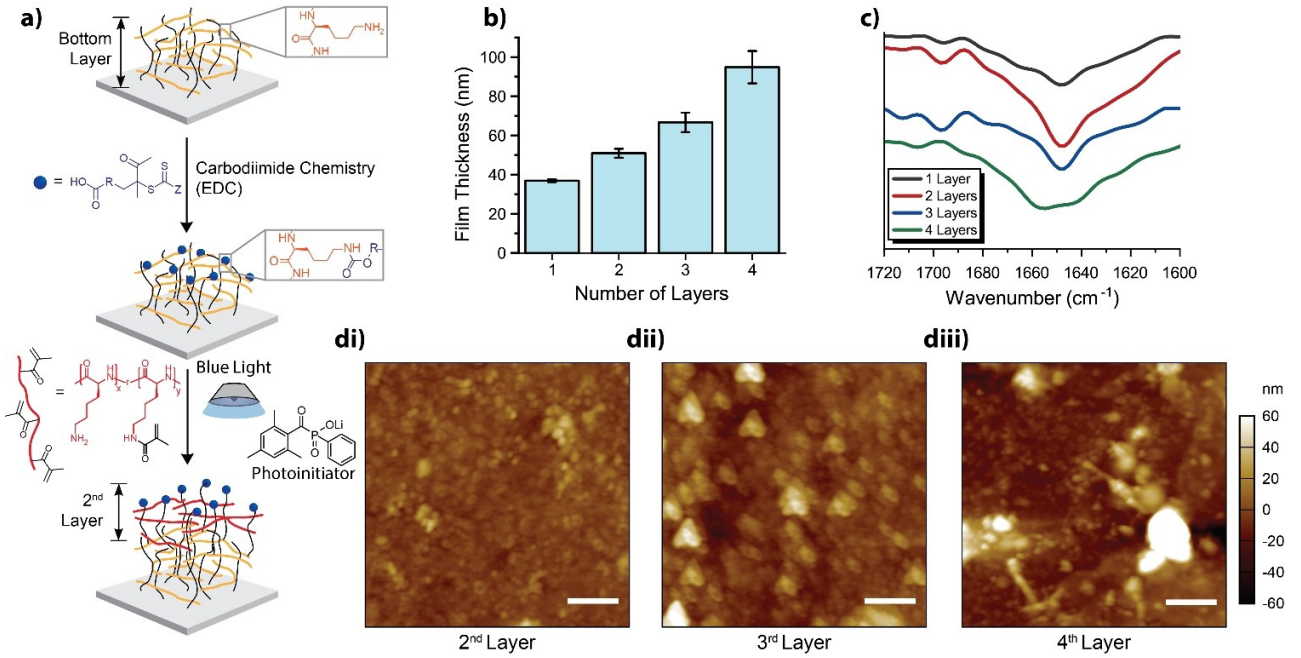

Figure 3. Multiple layers synthesized using CAP-RAFT. a) Schematic for reinitiation and execution of multiple layers of CAP-RAFT. b) Film thickness for multiple layers with PLLMA macrocrosslinker determined using AFM. c) FTIR spectra of the Amide I band of each layer. d) Surface morphology as revealed by AFM imaging of the di) 2nd, dii) 3rd and diii) 4th layers. (scale bars = 1 μm). EDC is 1-ethyl-3-(3-dimethylaminopropyl) carbodiimide.

tide directly to the surface showed this α-helical structure while in their uncharged state.[31] Subsequently, it might be reasonable to assume that since polylysine favors α-helices,[32] the films may form the same secondary structure. However, this was not the case when using CAP-RAFT as they instead preferentially formed random coils and β-sheets in the majority of the films (Table 1). While random coil content tended to vary significantly between 30 to 50 %, the β-sheet content remained between 32 to 39 %. This deviation from the expected α-helical structures is likely due to the unique covalently crosslinked morphology of films formed through CAP, resulting in reduced mobility of the PLLMA chains and thus preventing their usual favored conformation. Interestingly, the four-layer films seem to trend back towards the expected norm with β-sheet and random coil content dropping to 21 and 19 % respectively, while α-helical structure rose from around 13–19 % to 26 %. Furthermore, β-turns were observed in a far more significant quantity at 27 %. The issues stated before, pertaining to localized film growth, would also lead to lower crosslinking density. Subsequently, chain mobility would be increased, allowing the PLLMA chains to begin to take on their more favorable conformations. This unusually high random coil conformation grants these films a more amorphous structure which can assist with accessibility to functional groups or motifs desired for further surface modification or the specific binding of molecules making them a prime candidate for drug delivery or tissue engineering where such signaling molecules and molecular payloads are desired.

To further establish the versatility of this technique, poly(L-glutamic acid-r-L-lysine-g-methacrylate) (PLGMA) was investigated in a similar fashion as PLLMA (Supporting Information Figure S3, Table S3) with similarly modifiable functionable group side chains (i.e. carboxylic acids). By performing CAP with PLGMA in aqueous media, a slightly thicker film of 41.2 ± 1.4 nm was observed, possibly attributed to PLGMA's inability to undergo aminolysis (Figure 4a). However, the comparative increase in film thickness was more pronounced when CAP was performed on a reinitiated PLLMA layer with a jump to 76.0 ± 9.4 nm. Since the reaction was performed at pH 7 (deionized water), PLLMA and PLGMA layers exist in both the cationic and anionic forms. This would potentially result in ionic attraction of the layers accounting for the observed increased film thickness.

Despite one sample including a PLLMA layer below the PLGMA layer, both samples with PLGMA share similar FTIR spectra around the Amide I band (Figure 4b). Using the same logic as before, as poly-L-glutamic acid is expected to take predominantly random coil conformations at neutral pH,[33] the high random coil content of the PLGMA films (37 ± 2 %) is unsurprising, though there are still significant quantities of other secondary structures which might be due to localised confinement afforded by the unique morphology of CAP films. However, analogous to layer-by-layer (LbL) films fabricated from poly-L-glutamic acid and poly-L-lysine[34] our PLLMA/PLGMA films would be expected to form primarily β-sheet formations, due to polyionic complexation. In contrast, this was not observed and, instead, a similar secondary structure breakdown to the solely PLGMA films (with the exception of β-turns at 23 ± 14 %) was elucidated. It can be surmised that after the initial layer

Table 1: Secondary structure elements of multi-layered PLLMA and PLGMA films (determined using ATR-FTIR).

Layer Number 1 (bottom)	2	3	4 (top)	β-Sheets [%]	α-Helices [%]	Random Coils [%]	β-Turns [%]	Others[a] [%]
PLLMA	–	–	–	37±6	19±11	35±11	9±5	N/A
PLLMA	PLLMA	–	–	32±7	13±3	50±5	5±2	N/A
PLLMA	PLLMA	PLLMA	–	39±2	15±3	40±2	6±2	N/A
PLLMA	PLLMA	PLLMA	PLLMA	21±4	26±1	19±2	27±4	6±4
PLGMA	–	–	–	19±1	29±2	37±2	13±2	2±1
PLLMA	PLGMA	–	–	14±4	25±8	37±12	23±14	2±1

[a] In some cases, the amount of "other" secondary structure was negligible and thus denoted as "N/A".

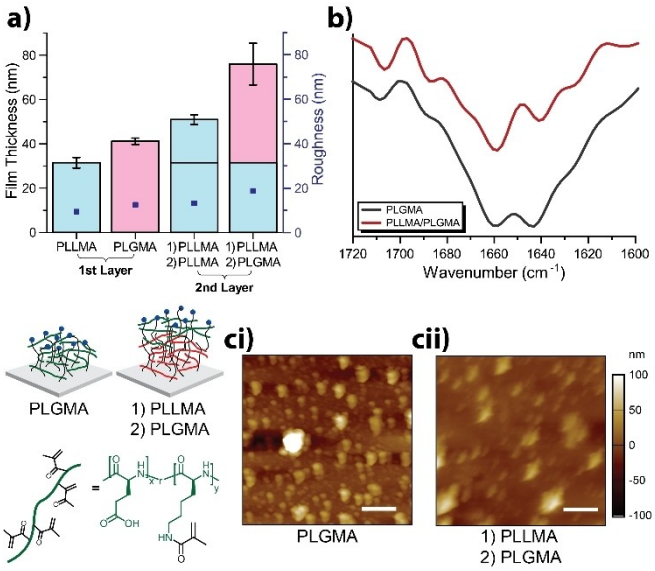

Figure 4. a) Comparative film thickness and roughness upon introduction of PLGlu as the initial layer and the second layer; b) FTIR spectra of top PLGlu layer; c) surface morphology of PLGlu layer as the ci) initial layer and cii) the second layer (scale bars = 1 μm).

of PLGMA, the subsequently deposited PLGMA layer no longer interacts strongly with the preceding PLLMA layer to form the polyionic complex as before.

Alongside their ability to form secondary structures, polypeptides are favourable in bio applications such as drug delivery and tissue engineering due to their ability to undergo enzymatic degradation.[35] To evaluate this susceptibility, the PLLMA- and PLGMA-based films were incubated with both α-chymotrypsin and protease type XIV as model proteases. α-chymotrypsin is a digestive enzyme present in the mammalian gut,[36] while protease type XIV is a protease mixture known to break down β-sheet structures and is often used in wound healing studies since it mimics the cocktail of metalloproteases (MMP's) found in wounds.[37] In general, proteases are expected to hydrolyse the amide bonds of the polypeptide backbone in multiple locations while leaving the hydrocarbon backbone formed through RAFT polymerization intact (Figure 5a). Thus, while it is expected that residual polymer remains, the majority of the film is degraded. AFM analysis of films at the same site of the PLLMA-based films before and after incubation (Figure 5b and d) revealed significant change using both enzymes. After the use of α-chymotrypsin, a noticeable increase in roughness was observed with both higher and lower regions of the films expanding relative to each other as a result of degradation in these lower regions in particular (Figure 5b). While this could also be observed in presence of protease type XIV (Figure 5d), a large piece was found missing after incubation indicating successful degradation. Interestingly, treatment of PLGMA films with these enzymes also yielded degradation, but it had little changes in the presence of α-chymotrypsin (Figure 5c), and none in the presence of protease type XIV showing resistance to this protease (Figure 5d). This suggests that degradation against certain enzymes can be controlled through selection of different amino acids though as is typical for proteases, since this control is enzyme specific. Thus, evidence of controllable enzymatic degradation has been demonstrated using both model enzymes, further suggesting potential in biological systems as scaffolds and drug delivery systems.

Conclusion

In summary, the first instance of CAP-RAFT has been established to form crosslinked polypeptide films with unique secondary structure features. Through the use of PLLMA as an initial model macrocrosslinker, investigations were performed with model dithiobenzoate and trithiocarbonate initiators and with and without sacrificial RAFT agent in solution. While the thickest films were obtained using surface confined dithiobenzoate RAFT agent (thickness of 36.1±1.1 nm), films of comparable thickness (31.5± 2.4 nm) and uniformity were obtained with sacrificial RAFT agent in solution. As a result, further experiments which ensured greater surface confinement were performed in the absence of RAFT agent in solution. In this way, multilayered films reaching a thickness of 94.9±8.24 nm were achieved. Secondary structure analysis showed an unusually high proportion of random coil structures (35–50 %), despite expected high α-helical formation for PLLMA. This is likely due to the reduced mobility of the surface confined PLLMA, and hence its ability to form the usually favored secondary structure. Similar trends were observed when the PLGMA macrocrosslinker was utilized. As a result, we have established CAP-RAFT as a viable strategy to create surface confined polypeptide crosslinked films with precision thick-

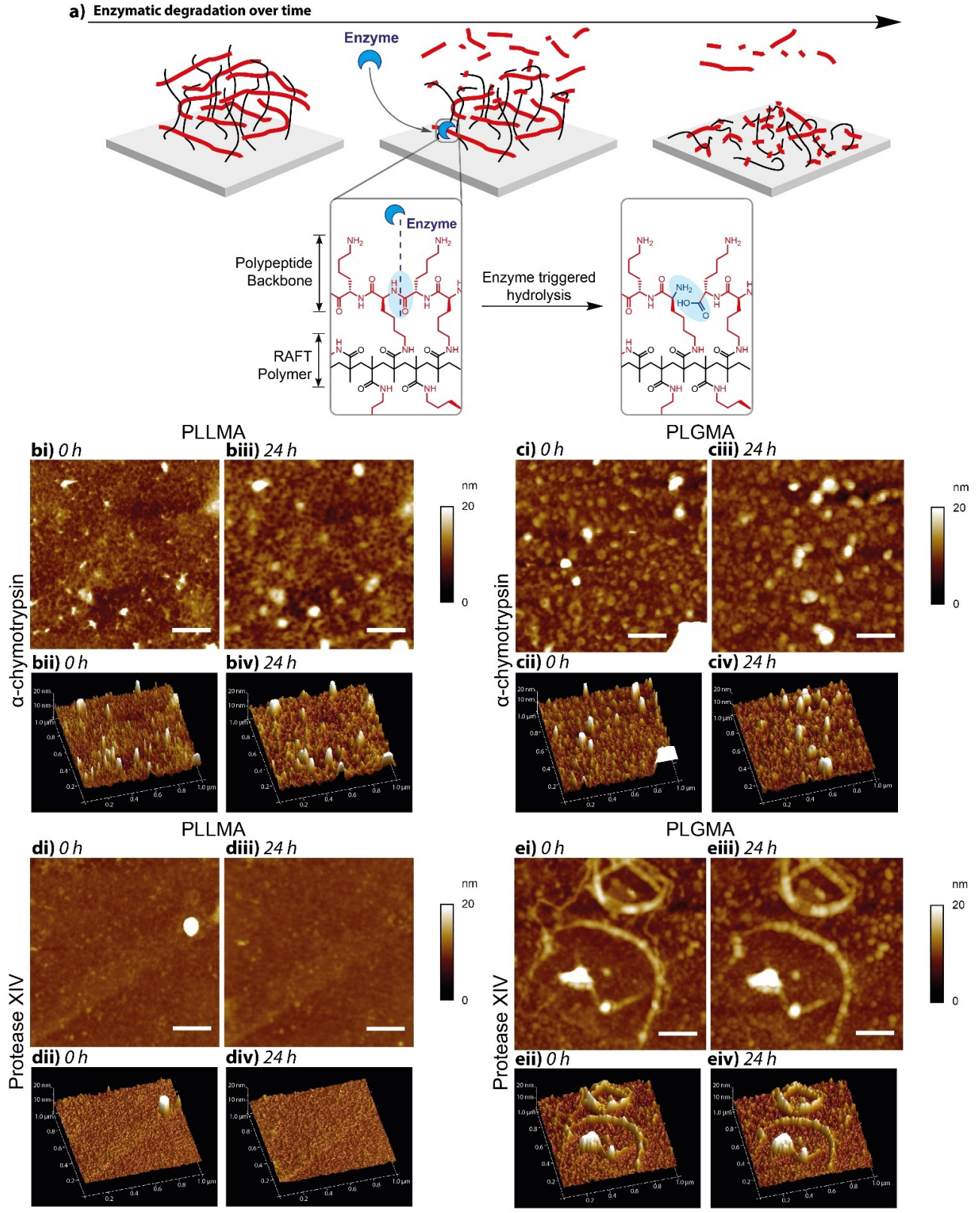

Figure 5. a) Schematic of enzymatic degradation of polypeptide films via hydrolysis of amide bonds in the polypeptide backbone (in red). Notably, the RAFT polymer remains intact (in black). b–e) AFM images of films treated with enzyme. b) PLLMA-based films before (bi, bii) and after incubation (biii, biv) with 1 mg mL^{-1} α-chymotrypsin at 25 °C. c) PLGMA-based films before (ci, cii) and after incubation (ciii, civ) with 1 mg mL^{-1} α-chymotrypsin at 25 °C. d) PLLMA-based films before (di, dii) and after incubation (diii, div) with 1 mg mL^{-1} Protease XIV at 37 °C. e) PLGMA-based films before (ei, eii) and after incubation (eiii, eiv) with 1 mg mL^{-1} Protease XIV at 37 °C. For b–e): 2D (i, iii) and 3D (ii, iv) image maps were utilized. Protease solutions used were 1 mg mL^{-1} α-chymotrypsin at 25 °C (b, c) and 1 mg mL^{-1} Protease XIV at 37 °C (d, e) (scale bars = 200 nm).

ness control and unique properties such as specific secondary structure formations and degradation. This secondary structure control combined with enzymatic degradation shows high potential for numerous biological applications including drug delivery and tissue engineering which will be subject to further investigation in future studies.

Acknowledgements

This work was performed in part at the Materials Characterization and Fabrication Platform (MCFP) at the University of Melbourne. We further thank Prof. Laforsch for access to the Harrick VariGATR. S.L thanks Markus Hund for technical assistance with AFM measurements. N.J.C thanks The University of Melbourne for providing Australian Government Research Training Program Scholarship (AGRTP) for providing funds for travel. This work is supported by grants DFG SCHE603/ 23-1. N.J.C., S.L., G.G.Q. and T.S. acknowledge funding from the German Academic Exchange Service (DAAD) through its thematic network Bayreuth-Melbourne Colloid/Polymer Network sponsored from funds of the Federal Ministry of Education and Research (BMBF). Open Access funding enabled and organized by Projekt DEAL.

Conflict of Interest

The authors declare no conflict of interest.

Keywords: CAP-RAFT · Crosslinked · Polypeptide · Surface-initiated polymerization · Secondary structure

[1] a) G. Bozokalfa, H. Akbulut, B. Demir, E. Guler, Z. P. Gumus, D. Odaci Demirkol, E. Aldemir, S. Yamada, T. Endo, H. Coskunol, S. Timur, Y. Yagci, *Anal. Chem.* **2016**, *88*, 4161–4167; b) B. Demir, T. Yilmaz, E. Guler, Z. P. Gumus, H. Akbulut, E. Aldemir, H. Coskunol, D. G. Colak, I. Cianga, S. Yamada, S. Timur, T. Endo, Y. Yagci, *Talanta* **2016**, *161*, 789–796; c) T. Yilmaz Sengel, E. Guler, Z. P. Gumus, E. Aldemir, H. Coskunol, H. Akbulut, D. Goen Colak, I. Cianga, S. Yamada, S. Timur, T. Endo, Y. Yagci, *Sens. Actuators B* **2017**, *246*, 310–318.

[2] a) K. Park, H. Jeong, J. Tanum, J.-C. Yoo, J. Hong, *J. Ind. Eng. Chem.* **2019**, *69*, 263–268; b) B. Jiang, B. Li, *Int. J. Nanomed.* **2009**, *4*, 37–53; c) B. Jiang, E. DeFusco, B. Li, *Biomacromolecules* **2010**, *11*, 3630–3637.

[3] a) Q. Gao, M. Yu, Y. Su, M. Xie, X. Zhao, P. Li, P. X. Ma, *Acta Biomater.* **2017**, *51*, 112–124; b) G. P. Sakala, M. Reches, *Adv. Mater. Interfaces* **2018**, *5*, 1800073; c) J. S. Rudra, K. Dave, D. T. Haynie, *J. Biomater. Sci. Polym. Ed.* **2006**, *17*, 1301–1315; d) Q. Yang, L. Wang, W. Lin, G. Ma, J. Yuan, S. Chen, *J. Mater. Chem. B* **2014**, *2*, 577–584.

[4] a) T. J. Deming, *J. Polym. Sci. Part A* **2000**, *38*, 3011–3018; b) T. J. Deming, *Nature* **1997**, *390*, 386–389; c) C. Nacar, *Protein J.* **2020**, *39*, 21–32; d) K. Fujiwara, H. Toda, M. Ikeguchi, *BMC Struct. Biol.* **2012**, *12*, 18.

[5] a) N. J.-A. Chan, D. Gu, S. Tan, Q. Fu, T. G. Pattison, A. J. O'Connor, G. G. Qiao, *Nat. Commun.* **2020**, *11*, 1630; b) D. T. Haynie, L. Zhang, J. S. Rudra, W. Zhao, Y. Zhong, N. Palath, *Biomacromolecules* **2005**, *6*, 2895–2913; c) S. H. Wibowo, A. Sulistio, E. H. H. Wong, A. Blencowe, G. G. Qiao, *Chem. Commun.* **2014**, *50*, 4971–4988; d) T. Borase, A. Heise, *Adv. Mater.* **2016**, *28*, 5725–5731.

[6] a) C. Zhang, J. Yuan, J. Lu, Y. Hou, W. Xiong, H. Lu, *Biomaterials* **2018**, *178*, 728–737; b) A. Heise, H. Menzel, H. Yim, M. D. Foster, R. H. Wieringa, A. J. Schouten, V. Erb, M. Stamm, *Langmuir* **1997**, *13*, 723–728; c) Y.-C. Chang, C. W. Frank, *Langmuir* **1996**, *12*, 5824–5829; d) F. Audouin, M. Fox, R. Larragy, P. Clarke, J. Huang, B. O'Connor, A. Heise, *Macromolecules* **2012**, *45*, 6127–6135.

[7] a) K. Kato, E. Uchida, E.-T. Kang, Y. Uyama, Y. Ikada, *Prog. Polym. Sci.* **2003**, *28*, 209–259; b) Y. Uyama, K. Kato, Y. Ikada, *Grafting/Characterization Techniques/Kinetic Modeling* **1998**, 1–39; c) M. Li, M. Fromel, D. Ranaweera, S. Rocha, C. Boyer, C. W. Pester, *ACS Macro Lett.* **2019**, *8*, 374–380.

[8] a) E. Roeven, A. R. Kuzmyn, L. Scheres, J. Baggerman, M. M. J. Smulders, H. Zuilhof, *Langmuir* **2020**, *36*, 10187–10199; b) Y. Zhang, K. Kang, N. Zhu, G. Li, X. Zhou, A. Zhang, Q. Yi, Y. Wu, *J. Mater. Chem. B* **2020**, *8*, 7428–7437.

[9] a) E. H. H. Wong, S. N. Guntari, A. Blencowe, M. P. van Koeverden, F. Caruso, G. G. Qiao, *ACS Macro Lett.* **2012**, *1*, 1020–1023; b) T. K. Goh, S. N. Guntari, C. J. Ochs, A. Blencowe, D. Mertz, L. A. Connal, G. K. Such, G. G. Qiao, F. Caruso, *Small* **2011**, *7*, 2863–2867; c) D. Mertz, C. J. Ochs, Z. Zhu, L. Lee, S. N. Guntari, G. K. Such, T. K. Goh, L. A. Connal, A. Blencowe, G. G. Qiao, F. Caruso, *Chem. Commun.* **2011**, *47*, 12601–12603; d) E. Nam, J. Kim, S. N. Guntari, H. Seyler, Q. Fu, E. H. H. Wong, A. Blencowe, D. J. Jones, F. Caruso, G. G. Qiao, *Chem. Sci.* **2014**, *5*, 3374–3380.

[10] a) S. N. Guntari, A. C. H. Khin, E. H. H. Wong, T. K. Goh, A. Blencowe, F. Caruso, G. G. Qiao, *Adv. Funct. Mater.* **2013**, *23*, 5159–5166; b) E. H. H. Wong, M. P. van Koeverden, E. Nam, S. N. Guntari, S. H. Wibowo, A. Blencowe, F. Caruso, G. G. Qiao, *Macromolecules* **2013**, *46*, 7789–7796; c) S. N. Guntari, T. K. Goh, A. Blencowe, E. H. H. Wong, F. Caruso, G. G. Qiao, *Polym. Chem.* **2013**, *4*, 68–75.

[11] a) Q. Fu, J. Kim, P. A. Gurr, J. M. P. Scofield, S. E. Kentish, G. G. Qiao, *Energy Environ. Sci.* **2016**, *9*, 434–440; b) E. Nam, E. H. H. Wong, S. Tan, Q. Fu, A. Blencowe, G. G. Qiao, *Macromol. Mater. Eng.* **2017**, *302*, 1600199.

[12] E. Nam, E. H. H. Wong, S. Tan, S. N. Guntari, Q. Fu, J. Kim, B. Delalat, A. Blencowe, G. G. Qiao, *Polym. Chem.* **2016**, *7*, 3251–3258.

[13] S. Tan, E. Nam, J. Cui, C. Xu, Q. Fu, J. M. Ren, E. H. H. Wong, K. Ladewig, F. Caruso, A. Blencowe, G. G. Qiao, *Chem. Commun.* **2015**, *51*, 2025–2028.

[14] T. G. Pattison, A. Spanu, A. M. Friz, Q. Fu, R. D. Miller, G. G. Qiao, *ACS Appl. Mater. Interfaces* **2020**, *12*, 4041–4051.

[15] a) G. Moad, E. Rizzardo, S. H. Thang, *Chem. Asian J.* **2013**, *8*, 1634–1644; b) G. Moad, *Polym. Chem.* **2017**, *8*, 177–219; c) M. D. Nothling, Q. Fu, A. Reyhani, S. Allison-Logan, K. Jung, J. Zhu, M. Kamigaito, C. Boyer, G. G. Qiao, *Adv. Sci.* **2020**, *7*, 2001656; d) G. Moad, E. Rizzardo, S. H. Thang, *Polymer* **2008**, *49*, 1079–1131; e) R. Whitfield, K. Parkatzidis, N. P. Truong, T. Junkers, A. Anastasaki, *Chem* **2020**, *6*, 1340–1352; f) K. Parkatzidis, H. S. Wang, N. P. Truong, A. Anastasaki, *Chem* **2020**, *6*, 1575–1588.

[16] a) S. Allison-Logan, F. Karimi, Y. Sun, T. G. McKenzie, M. D. Nothling, G. Bryant, G. G. Qiao, *ACS Macro Lett.* **2019**, *8*, 1291–1295; b) A. Reyhani, S. Allison-Logan, H. Ranji-Burachaloo, T. G. McKenzie, G. Bryant, G. G. Qiao, *J. Polym. Sci. Part A* **2019**, *57*, 1922–1930.

[17] a) A. R. Kuzmyn, A. T. Nguyen, L. W. Teunissen, H. Zuilhof, J. Baggerman, *Langmuir* **2020**, *36*, 4439–4446; b) Q. Wang, L. Hu, Z. Cui, P. Fu, M. Liu, X. Qiao, X. Pang, *ACS Appl. Mater. Interfaces* **2020**, *12*, 42161–42168.

[18] a) S. Allison-Logan, Q. Fu, Y. Sun, M. Liu, J. Xie, J. Tang, G. G. Qiao, *Angew. Chem. Int. Ed.* **2020**, *59*, 21392–21396; *Angew. Chem.* **2020**, *132*, 21576–21580; b) T. G. McKenzie, E. H. H. Wong, Q. Fu, A. Sulistio, D. E. Dunstan, G. G. Qiao, *ACS Macro Lett.* **2015**, *4*, 1012–1016.
[19] a) S. J. Lam, N. M. O'Brien-Simpson, N. Pantarat, A. Sulistio, E. H. H. Wong, Y.-Y. Chen, J. C. Lenzo, J. A. Holden, A. Blencowe, E. C. Reynolds, G. G. Qiao, *Nat. Microbiol.* **2016**, *1*, 16162; b) S. J. Shirbin, S. J. Lam, N. J.-A. Chan, M. M. Ozmen, Q. Fu, N. O'Brien-Simpson, E. C. Reynolds, G. G. Qiao, *ACS Macro Lett.* **2016**, *5*, 552–557.
[20] a) G. J. M. Habraken, K. H. R. M. Wilsens, C. E. Koning, A. Heise, *Polym. Chem.* **2011**, *2*, 1322–1330; b) Z. Song, Z. Tan, J. Cheng, *Macromolecules* **2019**, *52*, 8521–8539; c) G. J. M. Habraken, M. Peeters, C. H. J. T. Dietz, C. E. Koning, A. Heise, *Polym. Chem.* **2010**, *1*, 514–524.
[21] a) H. Lu, J. Wang, Z. Song, L. Yin, Y. Zhang, H. Tang, C. Tu, Y. Lin, J. Cheng, *Chem. Commun.* **2014**, *50*, 139–155; b) N. Hadjichristidis, H. Iatrou, M. Pitsikalis, G. Sakellariou, *Chem. Rev.* **2009**, *109*, 5528–5578.
[22] M. D. Nothling, T. G. McKenzie, I. A. Eastland, H.-C. Chien, J. Collins, A. S. Meyer, G. G. Qiao, *Chem. Commun.* **2019**, *55*, 8544–8547.
[23] a) Y. A. Vasilieva, C. W. Scales, D. B. Thomas, R. G. Ezell, A. B. Lowe, N. Ayres, C. L. McCormick, *J. Polym. Sci. Part A* **2005**, *43*, 3141–3152; b) P. Singhsa, H. Manuspiya, R. Narain, *Polym. Chem.* **2017**, *8*, 4140–4151.
[24] T. G. McKenzie, Q. Fu, E. H. H. Wong, D. E. Dunstan, G. G. Qiao, *Macromolecules* **2015**, *48*, 3864–3872.
[25] S. E. Seo, E. H. Discekici, Y. Zhang, C. M. Bates, C. J. Hawker, *J. Polym. Sci.* **2020**, *58*, 70–76.
[26] a) J. Xu, J. He, D. Fan, X. Wang, Y. Yang, *Macromolecules* **2006**, *39*, 8616–8624; b) C. Boyer, A. Granville, T. P. Davis, V. Bulmus, *J. Polym. Sci. Part A* **2009**, *47*, 3773–3794; c) G. B. Desmet, D. R. D'hooge, M. K. Sabbe, M.-F. Reyniers, G. B. Marin, *J. Org. Chem.* **2016**, *81*, 11626–11634.
[27] a) Y. Shi, E. T. A. van den Dungen, B. Klumperman, C. F. van Nostrum, W. E. Hennink, *ACS Macro Lett.* **2013**, *2*, 403–408; b) K. Luo, J. Yang, P. Kopečková, J. Kopeček, *Macromolecules* **2011**, *44*, 2481–2488.
[28] a) X. Zhou, Z. Li, *Adv. Healthcare Mater.* **2018**, *7*, 1800020; b) J. Huang, A. Heise, *Chem. Soc. Rev.* **2013**, *42*, 7373–7390; c) N. H. Lee, L. M. Christensen, C. W. Frank, *Langmuir* **2003**, *19*, 3525–3530; d) K. Cieślik-Boczula, *Biochimie* **2017**, *137*, 106–114.
[29] a) A. Barth, *Biochim. Biophys. Acta Bioenerg.* **2007**, *1767*, 1073–1101; b) Y. N. Chirgadze, B. V. Shestopalov, S. Y. Venyaminov, *Biopolymers* **1973**, *12*, 1337–1351.
[30] D. Huesmann, A. Birke, K. Klinker, S. Türk, H. J. Räder, M. Barz, *Macromolecules* **2014**, *47*, 928–936.
[31] a) A. Di Mauro, F. Mirabella, A. D'Urso, R. Randazzo, R. Purrello, M. E. Fragalà, *J. Colloid Interface Sci.* **2015**, *437*, 270–276; b) Y. Wang, Y. C. Chang, *Macromolecules* **2003**, *36*, 6511–6518.
[32] A. Mirtič, J. Grdadolnik, *Biophys. Chem.* **2013**, *175–176*, 47–53.
[33] K. Inoue, N. Baden, M. Terazima, *J. Phys. Chem. B* **2005**, *109*, 22623–22628.
[34] A.-M. Pilbat, V. Ball, P. Schaaf, J.-C. Voegel, B. Szalontai, *Langmuir* **2006**, *22*, 5753–5759.
[35] a) S. J. Shirbin, F. Karimi, N. J.-A. Chan, D. E. Heath, G. G. Qiao, *Biomacromolecules* **2016**, *17*, 2981–2991; b) M. Byrne, P. D. Thornton, S.-A. Cryan, A. Heise, *Polym. Chem.* **2012**, *3*, 2825–2831; c) M. K. Joo, D. Y. Ko, S. J. Jeong, M. H. Park, U. P. Shinde, B. Jeong, *Soft Matter* **2013**, *9*, 8014–8022.
[36] a) D. M. Blow, *Acc. Chem. Res.* **1976**, *9*, 145–152; b) W. Appel, *Clin. Biochem.* **1986**, *19*, 317–322.
[37] a) J. Brown, C.-L. Lu, J. Coburn, D. L. Kaplan, *Acta Biomater.* **2015**, *11*, 212–221; b) S. Müller-Herrmann, T. Scheibel, *ACS Biomater. Sci. Eng.* **2015**, *1*, 247–259.

Manuscript received: September 21, 2021
Accepted manuscript online: December 3, 2021
Version of record online: January 12, 2022